

FEM Modelling of Elastically Strained Interfacial Microstructures in Cu-Al-Ni Single Crystals

Ondřej GLATZ^{1,2}, Hanuš SEINER^{1,2,a}, and Michal LANDA¹

¹ Institute of Thermomechanics, Academy of Sciences of the Czech Republic, Dolejškova 5, 182 00 Prague 8, Czech Republic.

² Faculty of Nuclear Sciences and Physical Engineering, Czech Technical University in Prague, Trojanova 13, 120 00 Prague 2, Czech Republic.

Abstract. In this paper, a construction of FEM models of particular microstructures forming between austenite and mechanically stabilised 2H-martensite of the Cu-Al-Ni shape memory alloy is presented. Since these microstructures appearing during the shape recovery process (the so-called X-interfaces or the X-microstructures) are not global minimisers of the free energy, their mesoscopic morphology cannot be determined from any known thermodynamic extremal criterion, but must be taken directly from the experimental observations. For the elastic coefficients of both austenite and martensite phase of this alloy known from the ultrasonic measurements, such model enables determination of elastic strains within the microstructure and, thus, evaluation of the stored elastic energy in the microstructure. The model (implemented in COMSOL Multiphysics FEM environment) is applied to analyse interfacial microstructures observed experimentally in a prismatic bar of a single crystal of the examined alloy, and to find optimal morphology of this microstructure by means of the free energy (local) minimisation.

1 Introduction

Formation of the so-called X-interfaces between austenite and a single variant of martensite in single crystals of the shape memory alloys was firstly reported by Basinsky and Christian for the In-Th alloy [1]. In the Cu-Al-Ni alloy, formation of such interfacial microstructures was recently observed by the authors [2–4] during the shape recovery process (thermally induced transition from 2H-martensite into austenite).

As shown by Ruddock [5] for the In-Th alloy and by the authors [4] for Cu-Al-Ni, the X-interface does not, for the free boundary conditions, minimise the Helmholtz free energy of the crystal

$$W(T, \mathbf{y}) = \int_{\Omega} w(T(x), \mathbf{U}(\nabla \mathbf{y}(\mathbf{x}))) \, d\mathbf{x}, \quad (1)$$

(\mathbf{x} and \mathbf{y} are the reference and the deformed configurations, $\mathbf{U} = \sqrt{(\nabla \mathbf{y})^T \nabla \mathbf{y}}$ is the Bain matrix, T is the temperature and w is a multi-well free energy density) which is, according to the widely accepted theory of Ball and James [6], a necessary condition for a martensitic microstructure to form and be stable.

This paper continues and extends the FEM analysis of the elastic strains in the X-interfaces in Cu-Al-Ni single crystals presented by the authors in [4].

^a e-mail: hseiner@it.cas.cz

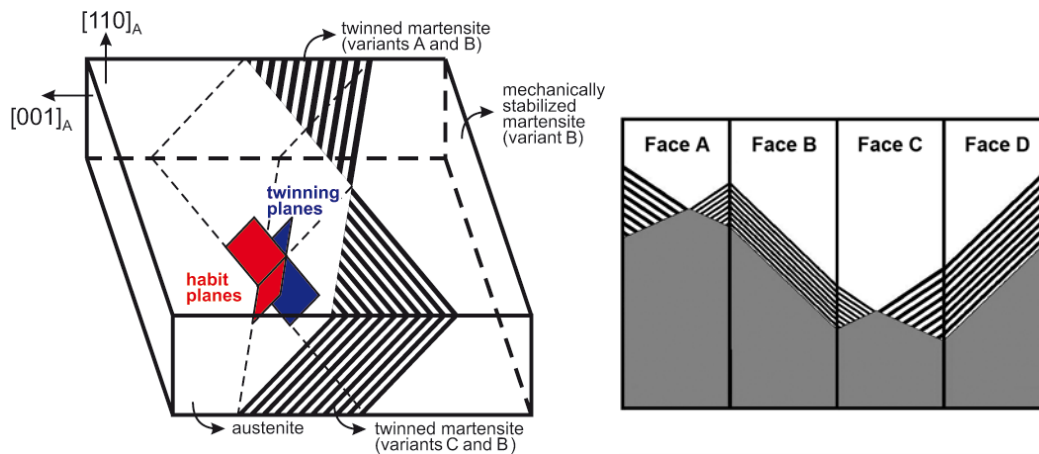


Fig. 1. X-microstructure scheme and faces notation.

2 The X-Microstructure

2.1 Experimentally observed X-interfaces

The X-interfaces were induced into a single crystal of Cu-Al-Ni (a rectangular, 15mm long prismatic bar with the axial direction close to $[001]$ in austenite and the lateral faces approximately perpendicular to $[110]$ and $[1\bar{1}0]$ directions in austenite) by the experimental procedure described in [3,4], i.e. by mechanical stabilisation and subsequent heating. The X-interfaces formed between the mechanically stabilised (2H) martensite and the austenitic region growing due to the heating.

The X-microstructure comprises austenite (I) and three variants of martensite (A, B, and C). It consists of two mutually intersecting habit planes (called AB habit plane and CB habit plane) separating austenite from twinned regions of martensite and another pair of mutually intersecting interfaces (called AB martensite–martensite interface and CB martensite–martensite interface) separating these twinned regions from the single variant of martensite. The martensite–martensite interfaces are parallel (or very close to parallel) to the twinning planes inside the corresponding twinned regions. The geometry of the X-microstructure is schematically sketched in Fig. 1. On the same figure also the notation of the faces can be found.

2.2 Compatibility Analysis

In order to analyse the compatibility, the particular variants of martensite and twinning systems appearing in the microstructure were identified. Optical micrographs of all faces of the specimen were taken and the angles (or more precisely their projections to particular faces) between the habit planes, twinning planes and the edges of the specimen were measured.

The Cu-Al-Ni alloy is a shape memory alloy undergoing a cubic to orthorhombic transition. For this kind of transition, the austenite phase can transform into six different variants of martensite. We denote these variants by numbers 1 to 6, and use the same numbering as in [7], where also the Bain matrices $U_{1,\dots,6}$ for these variants can be found.

A script written in MATLAB was used to compute orientations of habit planes and twinning planes of all possible combinations of variants, and to find which of these combinations fits the optical micrographs optimally. By this script, the twinning systems in the observed microstructure were identified as Type-II twinning planes of 2H martensite. The involved variants identified by this script are: No. 4 and No. 6 forming the AB twinning system and No. 2 and No. 6 forming the CB twinning system. This induces that the variant B of the pure martensite region (i.e. the variant involved in both laminates) must be No. 6, which was verified by X-ray measurements (Laue's method).

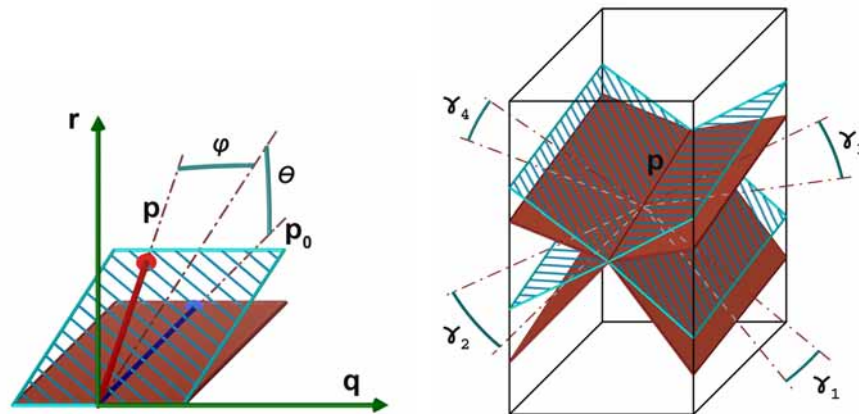


Fig. 2. Geometric parameters of the X-microstructure. The $(\gamma_1, \gamma_2, \gamma_3, \gamma_4, \theta, \varphi)$ are angles describing microstructure geometry. Vector \mathbf{p}_0 denotes direction of the intersecting line of the habit planes predicted by the classical theory, vector \mathbf{q} is aligned with the bottom edge of the face A, vector \mathbf{r} is perpendicular to \mathbf{q} and \mathbf{p}_0 . Vector \mathbf{p} is a new direction of the intersecting line.

Unfortunately, for such arrangement of variants the computed habit planes and martensite–martensite interfaces do not intersect exactly at one line. The difference between the intersecting line of the habit planes and the intersecting line of the martensite–martensite interfaces is 2.2° . Further, orientation of the common variant B in AB twinning system is different from the orientation in CB twinning system. Here, the difference in rotations is about 6.6° . Thus, although, the X-microstructure cannot exist in Cu–Al–Ni according to the classical theory, the incompatibilities are so small that they might be compensated by elastic deformation.

3 Modelling

As shown above, the X-microstructure cannot exist without presence of elastic strains. In this section we will try to determine stress fields for various geometry configurations and evaluate corresponding elastic energy.

Since the X-microstructure involves elastic strains, the respective minimizing sequence cannot be a global minimizer of stored Helmholtz free energy (1). Thus we propose a little modification of the classical theory [6]. The stable microstructure is supposed to be only a *local* minimiser of stored free energy. At the transition temperature, where the free energies of both phases in stress-free states are the same, this means that the sought geometry of the microstructure must minimise the elastic energy of the specimen.

To demonstrate this conjecture, we show by a FEM computation that the observed geometry of the microstructure corresponds to or lies very close to a local minimum of the elastic energy as a function of geometric parameters.

3.1 Problem Definition

First of all the suitable parametrisation of the geometry must be found. Dimensions of the specimen are fixed as well as position of the X-microstructure. Twinned regions are treated as homogeneous and interfaces are supposed to be exact planes. We choose austenite phase as a reference configuration.

From Section 2.2 it is clear that the intersecting line of habit planes and martensite–martensite interfaces is not well defined. Thus the direction \mathbf{p} of this line is our first geometric parameter. The direction is given by two angles θ and φ (see Fig. 2), which describe the deviation of this line from the direction \mathbf{p}_0 of intersection of the habit planes predicted by the

classical theory. Position of the line is given by one fixed point preventing the microstructure from moving through the specimen as a whole.

Remaining parameters are four angles ($\gamma_1, \gamma_2, \gamma_3, \gamma_4$) describing the orientations of two habit planes and two martensite–martensite interfaces (see Fig. 2). These angles represent deviations of respective planes from the reference planes, which are the planes closest to the corresponding planes predicted by the classical theory and containing intersecting line given by \mathbf{p} . The reference plane normal can be obtained as a vector triple product $\mathbf{p} \times (\mathbf{p} \times \mathbf{n}_0)$, where \mathbf{n}_0 is a normal vector from the classical theory. Then the whole geometry is described by six independent parameters. With all parameters set to zero the habit planes are exactly the habit planes predicted by the classical theory and martensite–martensite interfaces are the best approximations of classical twinning planes, which intersect with the habit planes in one common line.

With the geometry defined, the last thing we need is some knowledge of the materials elastic properties. Elastic constants of austenite and single variant of martensite are known from measurements (see [7]). The constants for the twinned regions are obtained by *homogenisation procedure* described in [8].

3.2 Model Solution

Our objective is to minimise elastic energy of the microstructure with respect to the chosen geometric parameters. Essential part of such optimization is the ability to evaluate strain fields and related elastic energy for the given geometry. In order to avoid problems with multiscale modelling the displacement field is decomposed into transformation and elastic parts. The nature of the martensitic phase transition enables us to understand it as two independent processes. The first is the deformation according to macroscopic gradients given by the material properties which yields to discontinuous displacement field over the incompatible interfaces, and the second is the elastic deformation which ensures the continuity of resulting displacements. Notice that both fields are discontinuous, but the composite of these is already continuous. The macroscopic deformation gradients corresponding to transformation part are taken from the classical theory. The elastic part of transition is to be found using FEM.

For the given geometry, the reference configuration is split to four regions. The first one remains in austenite after the transition, the second one transforms into single variant B of martensite, and remaining two transform into twinned martensites (AB, CB systems). For all of them, the macroscopic transformation strains are known. Since these strains in general are not compatible over the given planes, by applying the deformation described by this strains to respective regions the body breaks into four domains.

The above described (broken) configuration was used as a initial geometry for FEM computation. Boundary conditions ensuring the putting of these domains “back together” were prescribed and (providing elastic constants of all domains) the resulting elasticity problem was solved. As an optimization algorithm we used a standard sequential quadratic programming (SQP) implemented in MATLAB Optimization Toolbox. Generation of geometry and FEM computations were done in MATLAB environment in connection with Comsol Multiphysics (former FEMLAB), using Lagrange cubic 3D finite elements.

4 Results

The optimal microstructure geometry and the related elastic energy were determined for 33 positions of crossing point moving from the left to the right in the front face (Face A) of the specimen. Starting point for the optimization algorithm was always the zero vector. For all configurations the SQP algorithm converged pretty well, the required accuracy was attained within 6–8 iterations (about 60 evaluations of the objective function). Dependence of the elastic energy of the optimal geometry on the crossing point position is plotted in Fig. 3. For comparison, the plot of elastic energy corresponding to optimization starting points is included. In Fig. 4 the stress fields (von Mises stress) plots can be found for several positions of the microstructure.

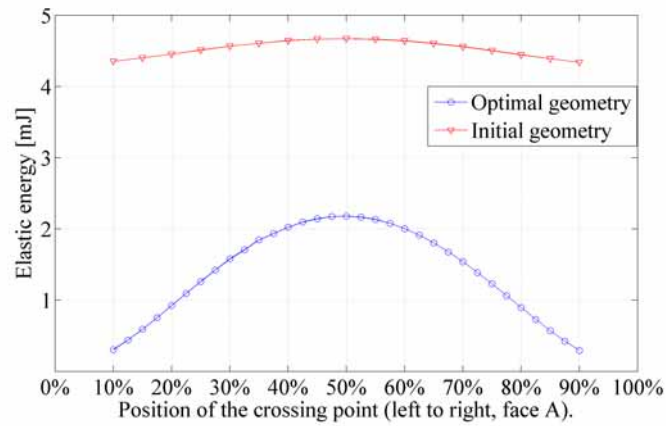


Fig. 3. Elastic energy as a function of crossing point position. Triangles—initial geometry; circles—optimal geometry.

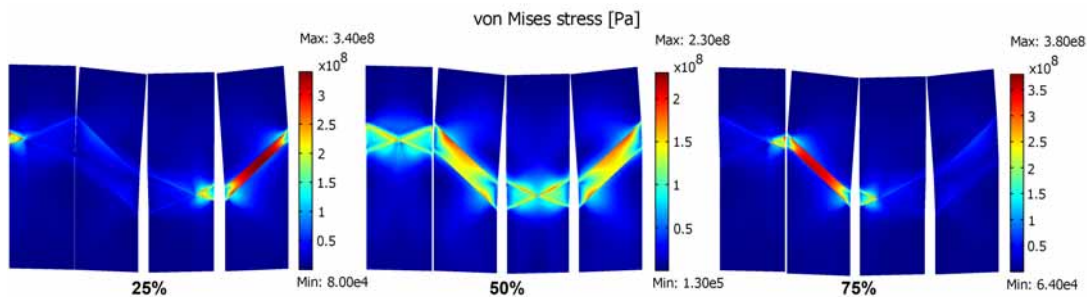


Fig. 4. Dependence of the stress distribution on the crossing point position.

Of course, the optimal geometry parameters varies with the position of the crossing point. The angle φ rises from -4° to 4° , the other parameters remain between 0° and 1° . For better understanding let us introduce new geometric parameters. These are the deviation angles projected to face A (alphas) and face B (betas) between the optimal planes and the planes predicted by the classical theory. For their dependence on the position of the crossing point see Fig. 5. Positive values mean counterclockwise rotation about the face A outer normal for alphas and face B outer normal for betas. We can conclude that the local minima of the elastic energy are very close the configurations predicted by the classical theory, and thus, the optimized morphologies are in a good agreement with the experimental observations.

5 Summary

In this paper, a mathematical model of the X-interfaces was constructed and used for determination of optimal geometries of these interfaces for given locations of the crossing lines (i.e. for a search for local minimizers of the Helmholtz free energy (1)). This model incorporated both the mesoscopic morphology of the interface (taken from the experiments) and the elastic strains necessary for the microstructure to achieve the compatibility (obtained by FEM calculations). The dependencies of individual geometric parameters of the microstructure (orientations of individual planar interfaces etc.) on the position of the crossing line were evaluated, showing that the optimized geometry does not deviate from the predictions of the classical theory [6] by more than 4° in orientations of individual planar interfaces.

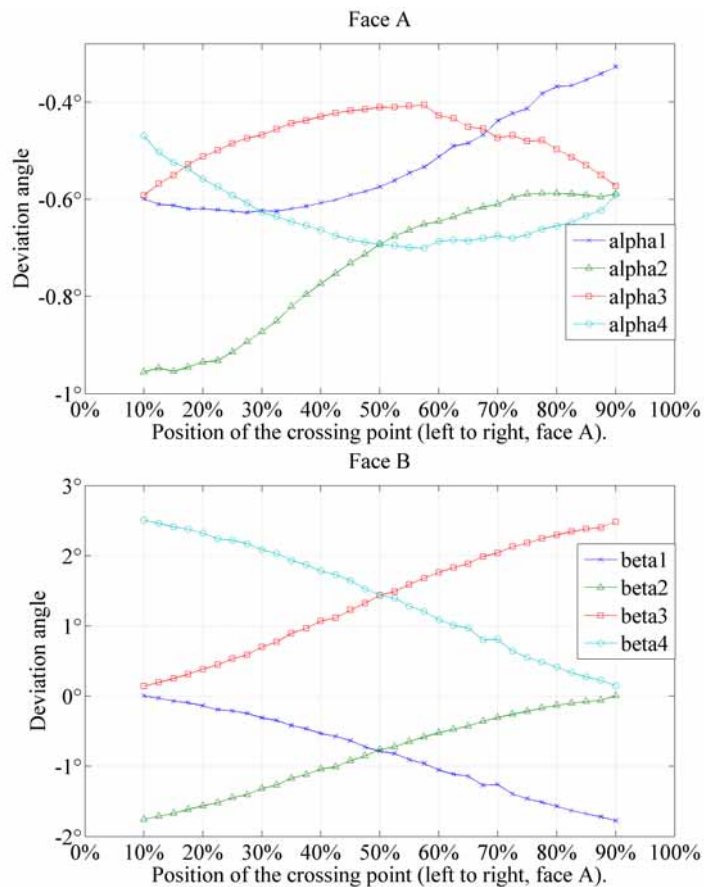


Fig. 5. Dependence of microstructure geometry on crossing point position. Deviations from the predicted planes in face A: α_1 —CB habit plane; α_2 —AB habit plane; α_3 —CB martensite–martensite interface; α_4 —AB martensite–martensite interface. Deviations from the predicted planes in face B: β_1 —CB habit plane; β_2 —AB habit plane; β_3 —CB martensite–martensite interface; β_4 —AB martensite–martensite interface.

Acknowledgment

This work was financially supported by project No.202/09/P164 of the Czech Science Foundation and by the institutional project of IT ASCR v.v.i. (CEZ:AV0Z20760514)

References

1. Basinski Z.S. and Christian J.W., *Acta Metallurgica* **2**, (1954) 102–106.
2. Seiner H., Landa M. and Sedláček P., *Proceedings of the Estonian Academy of Sciences* **56**,(2007) 218–225.
3. Seiner H., Sedláček P. and Landa M., *Phase transitions* **81**, (2008) 537–551.
4. Seiner H., Sedláček P. and Landa M., accepted to *International Journal for Multiscale Computational Engineering*, in production.
5. Ruddock G., *Archive for Rational Mechanics and Analysis* **127**, (1994) 1–39.
6. Ball J.M. and James R.D., *Archive for Rational Mechanics and Analysis* **100**, (1987) 13–52.
7. Sedláček P., Seiner H., Landa M., Novák V., Šittner P. and Manosa L., *Acta Materialia*, **53**, (2005), 3643–3661.
8. Landa M., Sedláček P., Seiner H., Heller L., Bicanová L., Šittner P., Novák V., *Applies Physics A*, in press.